RSC Advances

ROYAL SOCIETY OF CHEMISTRY

www.rsc.org/advances

Cite this: DOI: 10.1039/c0xx00000x

www.rsc.org/xxxxxx

ARTICLE TYPE

A crystalline molecular gyrotop with germanium junctions between a phenylene rotor and alkyl spokes†

Yusuke Inagaki,[a] Kentaro Yamaguchi,[b] and Wataru Setaka*[a]

Received (in XXX, XXX) Xth XXXXXXXXX 20XX, Accepted Xth XXXXXXXXX 20XX

DOI: 10.1039/b000000x

Macrocage molecules with a bridged phenylene have been reported as molecular gyrotops, in which the phenylene moiety can rotate even in the crystalline state. The roles of the atoms in the junctions between the rotor and spokes in molecular gyrotops have not been clarified well. In this study, a molecular gyrotop with germanium junctions was designed and synthesized, and the differences between the properties of the germanium and silicon derivatives were discussed. Notably, a structural isomer of the cage, which is not formed in the synthesis of the silicon derivative, was formed during the synthesis of the germanium derivative. Because the long Ge-C(Ph) bond length (1.958(4) Å) was observed in the crystal structure of the germanium derivative as compared to the Si-C(Ph) bond length (1.885(2) Å) of the silicon derivative, the activation energy for the rotation of the phenylene moiety inside the crystalline state of the germanium derivative (8.0 kcal/mol) was lower than that of the silicon derivative (9.0 kcal/mol). Similar tendencies of temperature-dependent optical properties of the single crystal, i.e., birefringence (Δn), were observed between the germanium and the silicon derivatives, but the temperatures and magnitudes of the discontinuous change in the birefringence were different.

Introduction

Because novel materials can be designed by controlling the internal molecular motion of artificial molecular rotors, the chemistry of such rotors has gained significant attention.[1-7] Specifically, macrocage molecules with a rotor inside their cages have been reported as crystalline molecular gyroscopes and gyrotops, because the rotor can rapidly rotate even in the crystalline state.[2-5] The chemistries of molecular gyroscopes and gyrotops in the crystalline state have been reported by Garcia-Garibay et al.,[2,6] Gladysz et al.,[3] and our group.[4,5] We synthesized molecular gyrotop **1** with a phenylene rotor with silicon junctions between the rotor and three alkyl spokes, and demonstrated the dynamics of the phenylene rotor in the crystalline state and the thermal changes in the birefringence of the single crystal.[4e] Chain-length (C_{14}-, C_{16}-, and C_{18}-chains) effects on the dynamic properties of molecular gyrotops have been reported recently,[4a] but the roles of atoms in the junctions have not been clarified.

In this study, molecular gyrotop **2** with germanium junctions was designed and synthesized. Since silicon and germanium are heavy group-14 elements, they exhibit similar properties. However, some properties are notably different. For instance, the mean bond length of Ge–C (1.95 Å) is longer than that of Si–C (1.88 Å);[8] hence, a lower rotational potential of the rotor in molecular gyrotop **2** is expected in comparison with the corresponding silicon derivative **1**.[4e] Furthermore, the reactivity of halogermane (R_xGeCl_{4-x}) is slightly different from that of halosilane (R_xSiCl_{4-x}).[8] In the present report, we discuss the differences between the structures and properties of the germanium (**2**) and silicon (**1**[4e]) derivatives of molecular gyrotops.

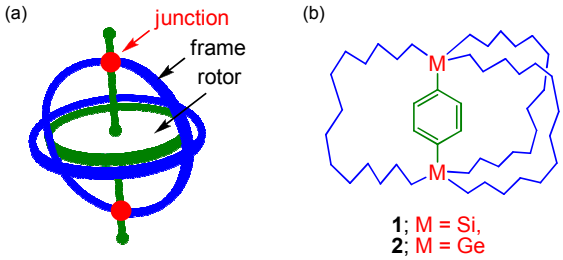

Scheme 1 (a) Gyrotop and (b) molecular gyrotops

Results and Discussion

I. Synthesis of the molecular gyrotop with germanium junctions (2)

The synthetic route toward molecular gyrotop **2** is shown in Scheme 2. The reaction between tetraethoxygermane with 3 equivalents of 7-octenyl magnesium bromide at 0 °C afforded ethoxytris(7-octenyl)germane (**3**) in 91% yield. In the substitution reaction of ethoxygermane ($Ge(OEt)_4$)[9] with Grignard reagents, it is possible to form mono-, di-, tri- and tetra-substituted products. Fortunately, the desired tri-substituted ethoxygermane was obtained as the sole product. Thus, further purification was not necessary after the removal of magnesium salts and solvents from the reaction mixture. Ethoxygermane **3** was quantitatively converted to the corresponding chlorogermane **4** upon reaction with acetyl chloride (AcCl). Notably, it is necessary to obtain chlorogermane **4** via ethoxygermane because the reaction of

$GeCl_4$ with 7-octenyl magnesium bromide at 0 °C did not yield the tri-substituted chlorogermane **4**. Digermylbenzene **5** was synthesized via the reaction of **4** with dilithiobenzene, which was prepared by reacting 1,4-dibromobenzene with *tert*-BuLi in tetrahydrofuran (THF) at –78 °C. The ring closing metathesis[10] of digermylbenzene in the presence of Grubbs' first-generation catalyst followed by hydrogenation with hydrogen gas at 3 atm in the presence of 10% Pd/C as a catalyst afforded the desired cage **2** along with a small amount of the corresponding structural isomer **2i**; they were easily separated by size exclusion chromatography. The molecular structures of these compounds were identified by NMR spectroscopy, elemental analyses, and X-ray crystallography. Cage **2** and isomer **2i** were formed in a 7:3 ratio. In contrast to the synthesis of silicon derivative **1**, where the structural isomer is not formed at all, the generation of the structural isomer in the synthesis of **2** can probably be attributed to the longer Ge-C bond.

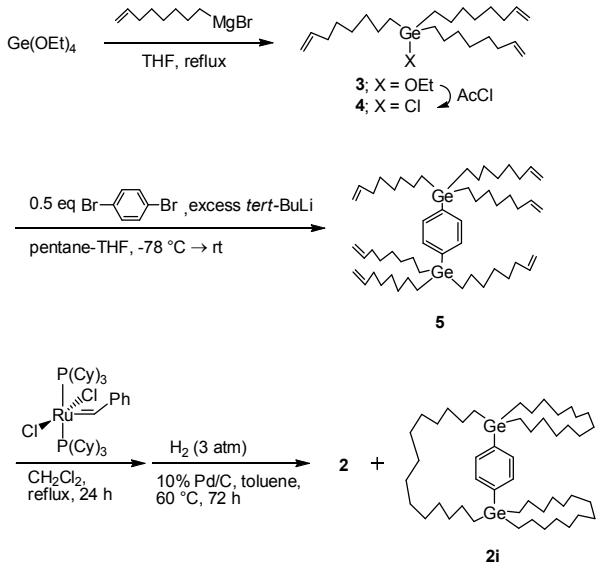

Scheme 2 Synthesis of molecular gyrotop **2**

II. Molecular structure of the molecular gyrotop (2)

The molecular structure of gyrotop **2** is shown in Fig 1, as determined by X-ray crystallography at 260 K. X-ray diffraction could not be carried out at temperatures below 260 K, because the single crystal, which was of a suitable size for X-ray diffraction, was cracked due to a phase transition that occurred at temperatures below 260 K. The molecular structure of germanium derivative **2** closely resembled silicon derivative **1**[4e], with the exception of the metal(Ge or Si)–carbon bond length. The cage structure of **2** was sphere-like, and effectively surrounded the phenylene rotor. The Ge-C(Ph) bond length (1.958(4) Å) of **2** was much longer than the Si-C(Ph) bond length (1.885(2) Å) of **1**[4e], and the observed structural features reflected the difference in the atomic size of Ge and Si.[8] The packing structures of **2** and **1**[4e] were also nearly identical owing to the same space group, and all molecules were arranged parallel to the rotation axis. Unfortunately, structural isomer **2i** could not be crystallized, and X-ray crystallography could not be carried out.

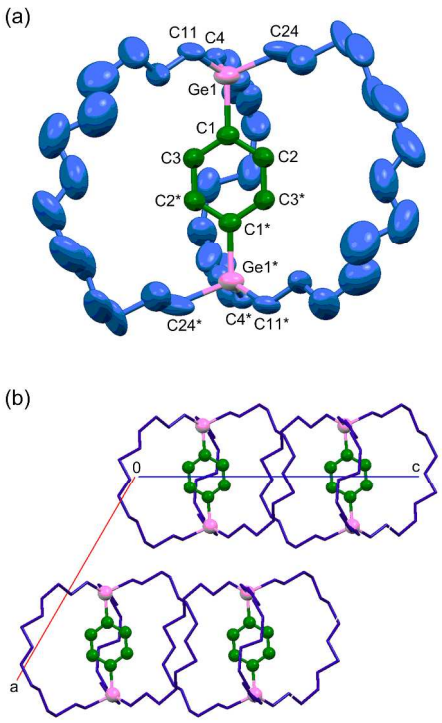

Fig. 1 Molecular structure of gyrotop **2** as determined by X-ray crystallography at 260 K. Hydrogen atoms and disordered atoms are omitted for clarity. (a) ORTEP drawing (30% thermal probability ellipsoid). Selected bond lengths (Å) and angles (º); Ge1-C1 1.958(4), Ge1-C1 1.957(5), Ge1-C4 1.929(6), Ge1-C11 1.850(13), Ge1-C24 2.041(11), C1-Ge1-C4 109.5(2); (b) Packing diagram of **2**.

III. Phenylene rotation of the molecular gyrotop (2) in the crystalline state

Phenylene rotation in the crystalline state was confirmed by solid-state ^{2}H NMR spectroscopy using the derivative with a deuterium-labeled phenylene rotor (**2**-d_4). Fig 2 shows the temperature-dependent solid-state ^{2}H NMR spectra of **2**-d_4. Broad signals due to quadruple coupling were observed.[11] The rotation of the phenylene moiety and the exchange rates can be estimated by simulations of the observed spectral line-shapes.[11] Fig 2 compares the observed and simulated spectra at each temperature. The simulated spectra of the phenylene moiety showed slow 180° flipping with exchange rate k below 240 K. At temperatures above 240 K, phenylene flipping with angular displacement Δ over the fast exchange limit (>3 MHz) was observed.[12] Here, the angular displacement Δ constitutes the range of the Gaussian distribution around the equilibrium position of the phenylene moiety. The dynamic features of the phenylene moiety in the crystalline state of germanium derivative **2** were similar to those of silicon derivative **1**;[4e] however, the temperature range in which the phenylene moiety showed slow flipping was slightly different. Specifically, the rotation of phenylene in **2** was more facile than that of **1**[4e] at the same temperature. Hence, lower activation energy for phenylene flipping of **2** than **1**[4e] was expected. In order to estimate the activation energy (E_a) for phenylene flipping, the temperature dependence of the spin-lattice relaxation times (T_1) of deuterium was investigated by solid-state ^{2}H NMR. T_1 can be

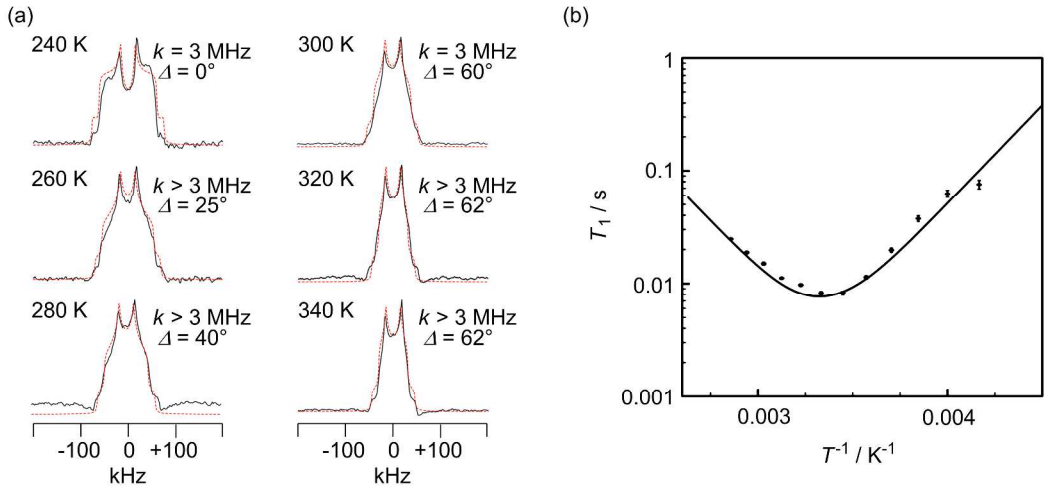

Fig. 2 (a) Temperature-dependent solid-state ^{2}H NMR spectra of **2**-d_4; observed spectra (solid black line); simulated spectra (dotted red line). Estimated exchange rate constant k and angular displacement Δ are shown. (b) Temperature-dependent ^{2}H spin-lattice relaxation times (T_1) in molecular gyrotop **2**-d_4. The lines are predicted based on the relaxation model (Eq. 1); the best fit parameters are as follows: $K = 4.41 \times 10^{10}$, $\tau_\infty = 2.0 \times 10^{-15}$ s, $E_a = 8.0$ kcal/mol.

fitted to the relaxation model (eq. 1), where the correlation time τ shows Arrhenius behavior.[13] Here, K is an effective coupling constant that depends on the quadruple coupling constant, and $\omega_0/2\pi$ is the Larmor frequency of deuterium.

$$\frac{1}{T_1} = K\left(\frac{\tau}{1+\omega_0^2\tau^2} + \frac{4\tau}{1+4\omega_0^2\tau^2}\right) \quad \text{, where } \tau = \tau_\infty \cdot e^{\frac{E_a}{RT}} \qquad \textbf{[1]}$$

Fig 2b shows a plot of the observed T_1 with the fitting curves calculated by eq. 1; the best fit parameters are described in the caption. The activation energy (E_a) of phenylene flipping was estimated to be 8.0 kcal/mol. The estimated Ea for phenylene flipping in **2** was lower than that of **1** (E_a = 9.0 kcal/mol[4e]) by 1.0 kcal/mol. These results indicated that the dynamics of the phenylene rotor of **2** and **1**[4e] were similar due to analogy in their molecular structures, and that the energy barriers for the flipping of **2** were lower than those of **1**[4e] due to long Ge–C(Ph) bonds.

IV. Birefringence of a single crystal of the molecular gyrotop (2)

Thermal changes in the birefringence of a single crystal of the silicon derivative of molecular gyrotop (**1**) were reported by our group recently.[4e] The birefringence is the difference between two refraction indices of the crystal, and the magnitude is known to depend on the structural anisotropy of the aggregates of atoms inside the crystal.[4e,14] Similar investigations were carried out for germanium derivative **2** in order to reveal the similarities and dissimilarities in the optical properties of single crystals of **1**[4e] and **2**. The crystal orientation of the widest face of a single crystal of **2** was determined to be {100} by X-ray diffraction at 300 K (Fig S24 in Supplementary Information), corresponding to the molecular aggregation inside the crystal, as indicated in Fig 3.

Fig 4 shows photographs of the single crystal of **2** on the {100} face at each temperature upon irradiation with polarized white light as observed by a polarized microscope; interference

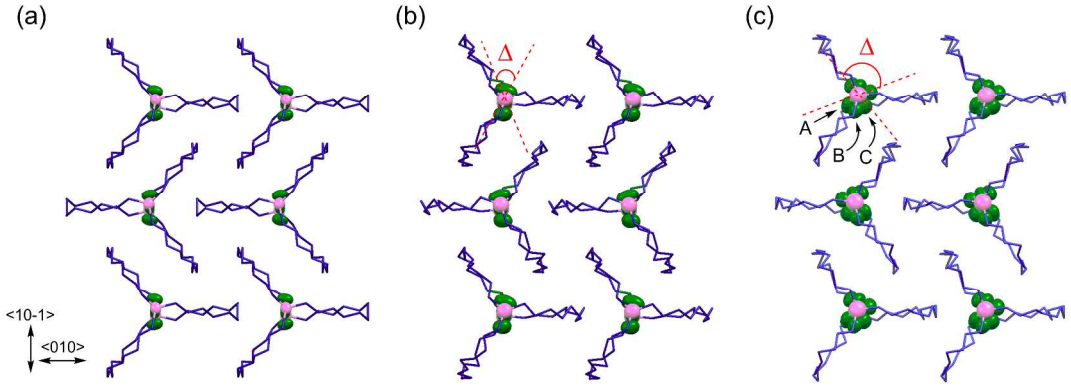

Fig. 3 Temperature-dependent crystal structure of molecular gyrotop **2** at (a) 260 K, (b) 300 K, and (c) 340 K. Figures were projected on the {100} face with the directions of the crystal orientation, disorder of the phenylene moiety, and angular displacement Δ. Germanium atoms and phenylene carbons are indicated with 50% probability ellipsoids. Population values of sites A, B, and C at 340 K were estimated to be 0.317(19), 0.50(2), and 0.190(14), respectively.

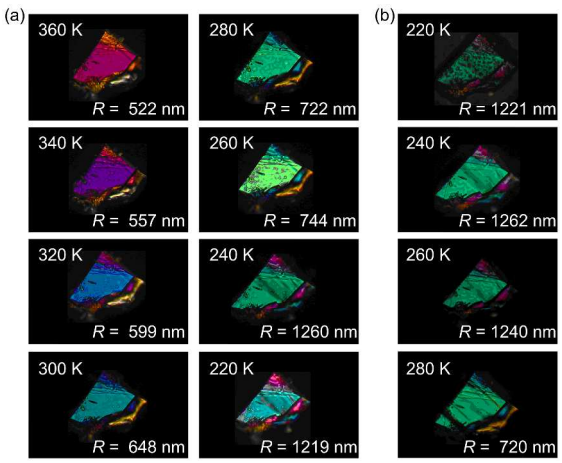

Fig. 4 Photographs of the single crystal of **2** on the {100} face upon irradiation with polarized white light, as observed by a polarized microscope (sample thickness: 64 μm, magnitude of the retardation is indicated); (a) cooling process; (b) heating process.

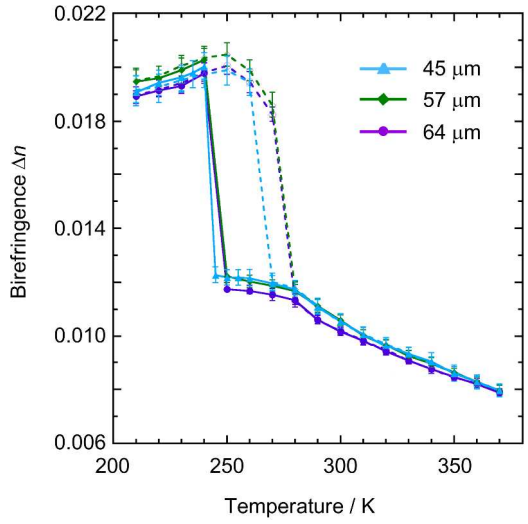

Fig. 5 Plots of birefringence (Δ*n*) versus temperature of **2** on the {100} face at 300 K; cooling process(solid lines); heating process (dotted lines).

colors were due to the retardation (*R*), of which the magnitude was obtained by multiplying the birefringence (Δ*n*) by the thickness of the sample (*d*). The interference colors gradually changed by cooling the sample from 360 K, and showed discontinuous change at 240 K (Fig 4(a)). In the heating process, the temperature of the phase transition changed (Fig 4(b)). Because the thickness (*d*) of the crystal was nearly unchanged in this temperature range, the variation in the interference color, i.e. retardation (*R*), was due to changes in the birefringence (Δ*n*) of the crystal.

Plots of the birefringence (Δ*n*) versus temperature (*T*) of several samples (*d* = 45, 57, and 64 μm measured at 300 K) of **2** are shown in Fig 5. The birefringence (Δ*n*) did not depend on the thickness of the samples, as the temperature-dependent birefringence (Δ*n*) of the samples was almost identical. At temperatures below the phase transition, the birefringence (Δ*n*) was almost constant at a relatively high value, whereas the magnitude of the birefringence (Δ*n*) decreased with increasing temperatures above the phase transition. Because the angular displacement (Δ) of the phenylene moiety inside the crystal was increased at high temperatures as determined by X-ray crystallography (Fig 3) and solid state NMR (Fig 2), the decrease of the birefringence (Δ*n*) above the phase transition was attributed to the averaging of the structural anisotropy inside the crystal. A similar temperature dependence of the birefringence was observed in a single crystal of silicon derivative **1**.[4e] As an additional evidence that the averaging of the structural anisotropy inside the crystal was the cause of the reduction of the birefringence, the slow axis of the refraction indices on the {100} face was found to be parallel to the phenylene plane of the molecular aggregate (see, Fig S27 in Supplementary Information). Moreover, birefringence (Δ*n*) hysteresis, whose width depended on the size of the crystal, was observed in germanium derivative **2**. The hysteresis indicates the process is the first-order phase transition. The small change of the birefringence around the hysteresis may be attributed to the strain of the single crystal. Notably, the interpretation of the absolute magnitude of the birefringence (Δ*n*) of single crystals remains unclear, and further investigations regarding the temperature-dependent birefringence (Δ*n*) of organic crystals are necessary in order to solve this problem.

Conclusions

We clarified the roles of the atoms in the junction by installing germanium atoms between the rotor and spokes in a molecular gyrotop. Because the long Ge-C(Ph) bond length (1.958(4) Å) was observed in the crystal structure of **2** as compared to the Si-C(Ph) bond length (1.885(2) Å) of **1**[4a,4e], the rotational barrier (E_a) for the rotation of the phenylene moiety inside the crystalline state of germanium derivative **2** (8.0 kcal/mol) was lower than that of the silicon derivative **1** (9.0 kcal/mol[4a,4e]). Similar tendencies of temperature-dependent optical properties of the single crystal, i.e., birefringence (Δ*n*), were observed between the germanium (**2**) and the silicon (**1**[4a,4e]) derivatives, but the temperatures and magnitudes of the discontinuous change in the birefringence were different..

Experimental Section

General All the reactions were carried out under an argon atmosphere. The chemical shifts of the ^{1}H (400 MHz) and ^{13}C (100 MHz) NMR spectra were calibrated using the resonance of the residual solvent. NMR signals were assigned by applying 1D and 2D NMR techniques (^{1}H, ^{13}C, DEPT, COSY, and HSQC). Commercially available reagents were used without further purification. Grubbs' catalysts, commercially available from Aldrich Chemicals, were used for the RCM reactions. Tetraethoxygermane ($Ge(OEt)_4$) was synthesized from tetrachlorogermane ($GeCl_4$) according to literature protocols.[9]

Synthesis of ethoxytris(7-octenyl)germane (3) A THF solution

(150 mL) of tetraethoxygermane (11.6 g, 45.9 mmol) was placed in a three-neck, flame-dried, round-bottom flask (500 mL) equipped with a magnetic stirrer, condenser, and dropping funnel. A THF solution of 7-octenyl magnesium bromide (100 mL) prepared from 7-octenylbromide (28.0 g, 146 mmol) and magnesium (3.79 g, 156 mmol) was introduced dropwise into the reaction flask cooled by an ice-water bath for 1 h. The reaction mixture was stirred at ambient temperature for 12 h. Volatile materials were removed in vacuo. Anhydrous pentane (≈ 200 mL) was added to the residual mixture, and magnesium salts were filtered using Celite. Evaporation of the filtrate afforded **3** (18.8 g, 91% yield) in 90% purity (determined by ^{1}H NMR spectroscopy). Further purification was not carried out owing to the compound's high boiling point and hydrolyzability. **3**: a pale yellow oil; ^{1}H NMR ($CDCl_3$, 400 MHz): δ 0.91-0.93 (m, 6H, Ge-CH_2-), 1.15 (t, J = 6.8 Hz, 3H, CH_3CH$_2$O), 1.28-1.41 (m, 24H), 2.01 (tddd, J = 6.5, 6.0, 1.1, 1.0 Hz, 6H, H$_2$C=CH-CH_2-), 3.61 (q, J = 6.8 Hz, 2H, CH$_3$CH_2O), 4.90 (ddt, J = 10.4, 2.4, 1.0 Hz, 3H, terminal H_2C=), 4.96 (ddt, J = 16.8, 2.4, 1.1 Hz, 3H, terminal H_2C=), 5.78 (ddt, J = 16.8, 10.4, 6.5 Hz, 6H, H$_2$C=CH-); ^{13}C NMR ($CDCl_3$, 100 MHz): δ 15.0, 19.4 (*C*H$_3$CH$_2$O), 24.0, 28.7, 28.8, 33.1, 33.8, 59.9 (CH$_3$*C*H$_2$O), 114.1 (-CH=*C*H$_2$), 139.1 (-*C*H=CH$_2$); Anal. Calcd for $C_{26}H_{56}GeO$: C, 69.19; H, 11.17. Found: C, 69.42; H, 11.24.

Synthesis of chlorotris(7-octenyl)germane (4) Ethoxytris(7-octenyl)germane (**3**, 8.0 g, 17.7 mmol) was placed in a two-neck, round-bottom flask (50 mL) equipped with a magnetic stirrer, condenser, and septum cap. Acetylchloride (9.7 g, 124 mmol) was introduced dropwise into the reaction flask through the septum cap by using a syringe. The reaction mixture was stirred at ambient temperature for 12 h. Volatile materials were removed under reduced pressure. Compound **9** (7.0 g, 89% yield) was obtained as a residual oil. Further purification of **9** was not carried out due to hydrolyzability. **4**: a pale yellow oil; ^{1}H NMR ($CDCl_3$, 400 MHz): δ 1.10-1.14 (m, 6H, Ge-CH_2-), 1.29-1.50 (m, 24H), 2.03 (tddd, J = 6.5, 6.0, 1.1, 1.0 Hz, 6H, H$_2$C=CH-CH_2-), 4.91 (ddt, J = 10.4, 2.4, 1.0 Hz, 3H, terminal H_2C=), 4.97 (ddt, J = 16.8, 2.4, 1.1 Hz, 3H, terminal H_2C=), 5.79 (ddt, J = 16.8, 10.4, 6.5 Hz, 3H, H$_2$C=CH-); ^{13}C NMR ($CDCl_3$, 100 MHz): δ 19.0, 24.0, 28.6, 28.8, 32.6, 33.8, 114.2 (-CH=*C*H$_2$), 139.0 (-*C*H=CH$_2$); Anal. Calcd for $C_{24}H_{45}GeCl$: C, 65.26; H, 10.27. Found: C, 65.07; H, 10.26.

Synthesis of 1,4-bis(tri-7-octenylgermyl)benzene (5) *p*-Dibromobenzene (1.6 g, 6.8 mmol) and dry THF (50 mL) were placed in a two-neck, round-bottom flask (100 mL) equipped with a magnetic stirrer and septum cap. A *tert*-BuLi solution (1.6 M in pentane, 17 mL, 4.0 equiv.) was added dropwise to the solution at –78 °C. The reaction mixture was stirred for an additional 3 h at –78 °C. It was then warmed up to –40 °C, and chlorogermane **4** (7.5 g, 17.0 mmol) was added. After stirring the mixture for 12 h at room temperature, it was hydrolyzed with dilute HCl (aq) and extracted with hexane. The organic layer was washed with saturated $NaHCO_3$ (aq) and dried over anhydrous Na_2SO_4. Concentration and subsequent column chromatography [Merck silica gel 60, particle size 63–200 μm, hexane/benzene = 4:1 as eluent (R_f = 0.77)] of the residue afforded **5** as a crude oil (4.49 g). Pure **5** (2.84 g, 3.20 mmol, 47% yield) was obtained after purification using gel permeation chromatography (GPC). **5**: a pale yellow oil; ^{1}H NMR ($CDCl_3$, 400 MHz): δ 0.95-0.99 (m, 12H, Ge-CH_2-), 1.32-1.39 (m, 48H), 2.04 (tddd, J = 6.5, 6.0, 1.1, 1.0 Hz, 12H, H$_2$C=CH-CH_2-), 4.94 (ddt, J = 10.4, 2.4, 1.0 Hz, 6H, terminal H_2C=), 5.00 (ddt, J = 16.8, 2.4, 1.1 Hz, 6H, terminal H_2C=), 5.81 (ddt, J = 16.8, 10.4, 6.5 Hz, 6H, H$_2$C=CH-), 7.38 (s, 4H, C$_6H_4$); ^{13}C NMR ($CDCl_3$, 100 MHz): δ 13.0, 25.1, 28.7, 28.9, 33.4, 33.8, 114.1 (-CH=*C*H$_2$), 133.2 (aromatic *C*H), 139.2 (Si*C*), 140.2 (-*C*H=CH$_2$); Anal. Calcd for $C_{54}H_{94}Ge_2$: C, 72.99; H, 10.66. Found: C, 73.05; H, 10.60.

Synthesis of molecular gyrotop 2 and its isomer 2i A dichloromethane solution (200 mL) of **5** (1.2 g, 1.35 mmol) was added dropwise with stirring over 12 h at 40 °C to a solution of dry dichloromethane (600 mL) in the presence of Grubbs' first-generation catalyst (0.02 g, 0.02 mmol). During the reaction, the catalyst (0.02 g, 0.06 mmol) was added to the flask twice. The mixture was stirred for an additional 8 h. Volatile materials were removed in vacuo, and the benzene-soluble fraction was subjected to flash column chromatography (silica gel, benzene) to remove the metal catalysts. The fraction contained unsaturated cyclized mixtures (0.8 g). After the mixture was subjected to GPC with chloroform as an eluent, two isomers (**6** (267 mg) and **6i** (91 mg)) with *E/Z*-alkenyl junctions were obtained. Then, hydrogen gas (3 atm) was introduced into a toluene (5 mL) solution of **6** in the presence of 10% Pd/C (0.03 g) in an autoclave, and the mixture was allowed to stand for 72 h at 60 °C. After excess H_2 gas was released, the mixture was filtered to remove Pd/C. Pure **2** (0.260 g, 0.321 mmol, 24% yield) was obtained after the removal of volatile materials in vacuo. Recrystallization of molecular gyrotop **2** from THF/MeOH (4/1 v/v) afforded single crystals of **2**. Pure **2i** (0.09 g, 0.111 mmol, 8% yield) was also obtained after hydrogenation of **6i** by the same method used for the synthesis of **2**.

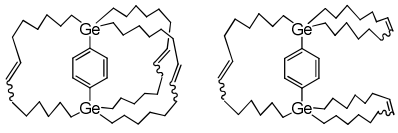

6 **6i**

Compound **2**: colorless crystals, mp 245.5–247.0 °C; ^{1}H NMR ($CDCl_3$, 400 MHz): δ 0.90-0.94 (m, 12H, Ge-CH_2-), 1.23-1.40 (m, 72H), 7.42 (s, 4H, aromatic CH); ^{13}C NMR ($CDCl_3$, 100 MHz): δ 13.5, 24.3, 27.83, 27.87, 28.5, 28.9, 32.4, 133.5 (aromatic CH), 139.5 (Ge*C*); Anal. Calcd. for $C_{48}H_{88}Ge_2$: C, 71.13; H, 10.94. Found: C, 71.07; H, 10.79. Compound **2i**: a colorless oil; ^{1}H NMR ($CDCl_3$, 400 MHz): δ 0.86-0.90 (m, 4H, Ge-CH_2-), 0.94-1.08 (m, 8H, Ge-CH_2-), 1.18-1.52 (m, 72H), 7.38 (s, 4H, aromatic CH); ^{13}C NMR ($CDCl_3$, 100 MHz): δ 12.6, 13.4, 23.9, 24.4, 26.4, 26.81, 26.83, 27.1, 27.7, 27.8, 28.1, 28.5, 31.5, 32.6, 133.2 (aromatic CH), 140.2 (SiC); Anal. Calcd. for $C_{48}H_{88}Ge_2$: C, 71.13; H, 10.94. Found: C, 70.92; H, 10.82.

Acknowledgements

This work was supported by a JSPS Grant-in-Aid for Scientific Research (B) (WS and KY, no. 25288042) and the Kurata Memorial Hitachi Science and Technology Foundation (WS).

Notes and references

[a] *Division of Applied Chemistry, Faculty of Urban Environmental Sciences, Tokyo Metropolitan University, 1-1 Minami-Osawa, Hachioji, Tokyo 192-0397, Japan. E-mail: wsetaka@tmu.ac.jp*

[b] *Faculty of Pharmaceutical Sciences at Kagawa Campus, Tokushima Bunri University, Sanuki, Kagawa 769-2193, Japan.*

† Electronic Supplementary Information (ESI) available: Copies of NMR spectra for all new compounds (**2**, **3**, **4**, **5**, and **2i**). Details of solid-state ^{2}H NMR Study of **2**-d_4. Details of temperature-dependent birefringence study of the single crystal of **2**. For ESI and crystallographic data or other electronic format. See DOI: 10.1039/b000000x/

‡ Crystallographic Data for **2** at 260 K: monoclinic, *C*2/*c*, a = 25.736(7) Å, b = 11.733(3) Å, c = 18.790(5) Å, β = 120.046(3)°, V = 4911(2) Å^3, $R1$ = 0.0640 ($I > 2\sigma I$), $wR2$ = 0.2352 (all data). Data at 300 K: monoclinic, *Cc*, a = 26.056(10) Å, b = 11.558(4) Å, c = 19.190(7) Å, β = 118.979(4)°, V = 5056(3) Å^3, $R1$ = 0.0712 ($I > 2\sigma I$), $wR2$ = 0.2628 (all data). Data at 340 K: monoclinic, *Cc*, a = 26.170(17) Å, b = 11.561(8) Å, c = 19.398(13) Å, β = 118.837(7)°, V = 5141(6) Å^3, $R1$ = 0.0585 ($I > 2\sigma I$), $wR2$ = 0.2312 (all data). The crystallographic data were deposited in the Cambridge Crystallographic Database Centre (CCDC-1026017 for 260 K, CCDC-1026018 for 300 K, and CCDC-1026019 for 340 K).

1 (a) C. S. Vogelsberg, M. A. Garcia-Garibay, *Chem. Soc. Rev.*, 2012, **41**, 1892; (b) A. R Karim, A. Linden, K. K. Baldridge, J. S. Siegel, *Chem. Sci*., 2010, **1**, 102; (c) V. Blanzani, A. Credi, M. Venturi, *Molecular Devices and Machines*, 2nd Edition, Wiley-VCH: Weinheim, 2008. (d) E. R. Kay, D. A. Leigh, F. Zerbetto, *Angew. Chem. Int. Ed,* 2007, **46**, 72; (e) W. R. Browne, B. L. Feringa, *Nature Nanotech.*, 2006, **1**, 25; (f) T. R. Kelly, *Molecular Machines. Topics in Current Chemistry,* Vol. 262, Springer: Hidelberg, 2005; (g) G. S. Kottas, L. I. Clarke, D. Horinek, J. Michl, *Chem. Rev.*, 2005, **105**, 1281; (h) M. A. Garcia-Garibay, *Proc. Nat. Acad. Sci. USA*, 2005, **102**, 10771; (i) V. Balzani, A. Credi, F. M. Raymo, J. F. Stoddart, *Angew. Chem. Int. Ed.,* 2000, **39**, 3348.

2 (a) P. Commins; M. A. Garcia-Garibay, *J. Org. Chem.* 2014, **79**, 1611; (b) P. Commins, J. E. Nuñez, M. A. Garcia-Garibay, *J. Org. Chem*., 2011, **76**, 8355; (c) J. E. Nuñez, A. Natarajan, S. I. Khan, M. A. Garcia-Garibay, *Org. Lett*., 2007, **9**, 3559.

3 (a) A. J. Nawara-Hultzsch, M. Stollenz, M. Barbasiewicz, S. Szafert, T. Lis, F. Hampel, N. Bhuvanesh, J. A. Gladysz, *Chem. Eur. J.*, 2014, **20**, 4617; (b) P. D. Zeits, G. P. Rachiero, F. Hampel, J. H. Reibenspies, J. A. Gladysz, *Organometallics*, 2012, **31**, 2854; (c) K. Skopek, J. A. Gladysz, *J. Organomet. Chem*., 2008, **693**, 857; (d) K. Skopek, M. Barbasiewicz, H. Hampel, J. A. Gladysz, *Inorg. Chem*., 2008, **47**, 3474; (e) J. Han, C. Deng, R. Fang, D. Zao, L. Wang, J. A. Gladysz, *Organometallics*, 2010, **29**, 3231; (f) G. D. Hess, F. Hampel, J. A. Gladysz, *Organometallics*, 2007, **26**, 5129; (g) L. Wang, T. Shima, F. Hampel, J. A. Gladysz, *Chem. Commun*., 2006, 4075; (h) L. Wang, F. Hampel, J. A. Gladysz, *Angew. Chem. Int. Ed.*, 2006, **45**, 4372; (i) A. J. Nawara, T. Shima, F. Hampel, J. A. Gladysz, *J. Am. Chem. Soc.*, 2006, **128**, 4962; (j) T. Shima, F. Hampel, J. A. Gladysz, *Angew. Chem. Int. Ed.*, 2004, **43**, 5537.

4 (a) W. Setaka, K. Inoue, S. Higa, S. Yoshigai, H. Kono, K. Yamaguchi, *J. Org. Chem.*, 2014, **79**, 8288; (b) W. Setaka, S. Higa, K. Yamaguchi, *Org. Biomol. Chem.*, 2014, **12**, 3354; (c) W. Setaka, K. Yamaguchi, *J. Am. Chem. Soc.*, 2013, **135**, 14560; (d) W. Setaka, A. Koyama, K. Yamaguchi, *Org. Lett*., 2013, **15**, 5092; (e) W. Setaka, K. Yamaguchi, *Proc. Natl. Acad. Sci. U.S.A.*, 2012, **109**, 9271; (f) W. Setaka, K. Yamaguchi, *J. Am. Chem. Soc.*, 2012, **134**, 12458.

5 (a) W. Setaka, S. Ohmizu, M. Kira, *Chem. Commun.*, 2014, **50**, 1098; (b) A. B. Marahatta, M. Kanno, K. Hoki, W. Setaka, S. Irle, H. Kono, *J. Phys. Chem. C*, 2012, **116**, 24845; (c) W. Setaka, S. Ohmizu, M. Kira, *Chem. Lett*., 2010, **39**, 468; (d) W. Setaka, S. Ohmizu, C. Kabuto, M. Kira, *Chem. Lett*., 2007, **36**, 1076.

6 (a) Z. Dominguez, H. Dang, M. J. Strouse, M. A. Garcia-Garibay, *J. Am. Chem. Soc.*, 2002, **124**, 2398; (b) C. E. Godinez, G. Zepeda, M. A. Garcia-Garibay, *J. Am. Chem. Soc.*, 2002, **124**, 4701; (c) Z. Dominguez, H. Dang, M. J. Strouse, M. A. Garcia-Garibay, *J. Am. Chem. Soc.*, 2002, **124**, 7719; (d) Z. Dominguez, T.-A. V. Khuong, C. H. Dang, N. Sanrame, J. E. Nuñez, M. A. Garcia-Garibay, *J. Am. Chem. Soc.,* 2003, **125**, 8827; (e) R. D. Horansky, L. Clarke, E. B. Winston, J. C. Price,S. D. Karlen, P. D. Jarowski, R. Santillan, M. A. Garcia-Garibay, *Phys. Rev. B,* 2006, **74**, 054306; (f) R. D. Horansky, L. I. Clarke, J. C. Price, T.-A. V. Khuong, P. D. Jarowski, M. A. Garcia-Garibay, *Phys. Rev. B,* 2005, **72**, 014302; (g) C. S. Vogelsberg, S. Bracco, M. Beretta, A. Comotti, P. Sozzani, M. A. Garcia-Garibay, M. A. *J. Phys. Chem. B*, 2012, **116**, 1623; (h) D. Czajkowska-Szczykowska, B. Rodríguez-Molina, N. E. Magaña-Vergara, R. Santillan, J. W. Morzycki, M. A. Garcia-Garibay, *J. Org. Chem.*, 2012, **77**, 9970; (i) B. Rodríguez-Molina, S. Pérez-Estrada, M. A. Garcia-Garibay, *J. Am. Chem. Soc.*, 2013, **135**, 10388; (j) B. Rodríguez-Molina, M. E. Ochoa, M. Romero, S. I. Khan, N. Farfán, R. Santillan, M. A. Garcia-Garibay, *Cryst. Growth Des*., 2013, **13**, 5107; (k) A. Torres-Huerta, B. Rodríguez-Molina, H. Höpfl, M. A. Garcia-Garibay, *Organometallics*, 2014, **33**, 354; (l) X. Jiang, B. Rodríguez-Molina, N. Nazarian, M. A. Garcia-Garibay, *J. Am. Chem. Soc.*, 2014, *136*, 8871.

7 (a) G. Bastien, C. Lemouchi, P. Wzietek, S. Simonov, L. Zorina, A. Rodríguez-Fortea, E. Canadell, P. Batail, *Anorg. Allg. Chem.*, 2014, **640**, 1127; (b) C. Lemouchi, H. M. Yamamoto, R. Kato, S. Simonov, L. Zorina, A. Rodríguez-Fortea, E. Canadell, P. Wzietek, K. Iliopoulos, D. Gindre, M. Chrysos, P. Batail, *Cryst. Growth Des*., 2014, **14** , 3375; (c) A. Comotti, S. Bracco, A. Yamamoto, M. Beretta, T. Hirukawa, N. Tohnai, M. Miyata, P. Sozzani, *J. Am. Chem. Soc.*, 2014, **136**, 618p; (d) C. Lemouchi, K. Iliopoulos, L. Zorina, S. Simonov, P. Wzietek, T. Cauchy, A. Rodríguez-Fortea, E. Canadell, J. Kaleta, J. Michl, D. Gindre, M. Chrysos, P. Batail, *J. Am. Chem. Soc.*, 2013, **135**, 9366.

8 C. Elschenbroich, *Organometallics*, Wiley-VCH, Weinheim, 2006, chapter 8.

9 P. Mazerolles, F. Grégoire, F. *Synthesis and Reactivity in Inorganic and Metal-Organic Chemistry,* 1986, **16**, 905.

10 (a) J. W. Herndon, *Coord. Chem. Rev.*, 2014, **272**, 48; (b) A. Fürstner, *Science*, 2013, **341**, 1229713; (c) R. H. Grubbs, in *Handbook of metathesis*, ed. R. H. Grubbs, Wiley-VCH, Weinheim, 2003, vol. 1–3; (d) R. R. Schrock, *Angew. Chem. Int. Ed*., 2006, **45**, 3748; (e) R. H. Grubbs, *Angew. Chem. Int. Ed*., 2006, **45**, 3760; (f) G. C. Vougioukalakis, R. H. Grubbs, *Chem. Rev*., 2010, **110**, 1746.

11 (a) G. L. Hoatson, R. L. Vold, *NMR Basic Principles Prog*., 1994, **32**, 1; (b) H. W. Spiess, *Colloid Polym. Sci*., 1983, **261**, 193; (c) J. H. Simpson, D. M. Rice, F. E. Karasz, *J. Polym. Sci. Part B*, 1992, **30**, 11; (d) A. L. Cholli, J. J. Dumais, A. K. Engel, L. W. Jelinski, *Macromolecules*, 1984, **17**, 2399.

12 (a) V. Macho, L. Brombacher, H. W. Spiess, *Appl. Magn. Reson.*, 2001, **20**, 405; (b) M. R. Hansen, R. Graf, H. W. Spiess, *Acc. Chem. Res.*, 2013, **46**, 1996; (c) K. Schmidt-Rohr, H. W. Spiess, *Multidemensional Solid-State NMR and Polyners*, Academic Press, London, 1994.

13 H. W. Spiess, *NMR Basic Principles and Progress*, Eds. P. Diehl, E. Fluck, R. Kosfeld, Springer, Heidelberg, 1978.

14 (a) M. Horie, Y. Suzaki, D. Hashizume, T. Abe, T. Wu, T. Sassa, T. Hosokai, K Osakada, *J. Am. Chem. Soc.*, 2012, **134**, 17932; (b) M. Horie, T. Sassa, D. Hashizume, Y. Suzaki, K. Osakada, T. Wada, *Angew. Chem. Int. Ed*.**,** 2007, **46**, 4983.

A molecular gyrotop with germanium junctions was synthesized, and the dynamics of the phenylene and the optical properties were discussed.